IOP Publishing Measurement Science and Technology
Meas. Sci. Technol. **25** (2014) 105011 (8pp) doi:10.1088/0957-0233/25/10/105011

Adaptive robust Kalman filtering for precise point positioning

Fei Guo and Xiaohong Zhang

School of Geodesy and Geomatics, Wuhan University, 129 Luoyu Road, Wuhan 430079, People's Republic of China

E-mail: fguo@sgg.whu.edu.cn and xhzhang@sgg.whu.edu.cn

Received 4 March 2014, revised 6 July 2014
Accepted for publication 18 July 2014
Published 15 September 2014

Abstract

The optimality of precise point postioning (PPP) solution using a Kalman filter is closely connected to the quality of the *a priori* information about the process noise and the updated mesurement noise, which are sometimes difficult to obtain. Also, the estimation enviroment in the case of dynamic or kinematic applications is not always fixed but is subject to change. To overcome these problems, an adaptive robust Kalman filtering algorithm, the main feature of which introduces an equivalent covariance matrix to resist the unexpected outliers and an adaptive factor to balance the contribution of observational information and predicted information from the system dynamic model, is applied for PPP processing. The basic models of PPP including the observation model, dynamic model and stochastic model are provided first. Then an adaptive robust Kalmam filter is developed for PPP. Compared with the conventional robust estimator, only the observation with largest standardized residual will be operated by the IGG III function in each iteration to avoid reducing the contribution of the normal observations or even filter divergence. Finally, tests carried out in both static and kinematic modes have confirmed that the adaptive robust Kalman filter outperforms the classic Kalman filter by turning either the equivalent variance matrix or the adaptive factor or both of them. This becomes evident when analyzing the positioning errors in flight tests at the turns due to the target maneuvering and unknown process/measurement noises.

Keywords: adaptive robust Kalman filtering, precise point positioning, equivalent covariance matrix, adaptive factor, maneuvering, dynamic model

(Some figures may appear in colour only in the online journal)

1. Introduction

Precise point positioning (PPP) has constantly been a research focus of the Global Navigation Satellite System (GNSS) community in the past decade. Normally, PPP utilizes dual-frequency GNSS data such as carrier phases and pseudoranges to conduct absolute precise positioning tasks at a single station, when precise satellite ephemeris and clock errors are provided and all the remaining unmodeled errors are addressed [16, 30]. It has been demonstrated to be a powerful tool in geodesy and geodynamic applications such as precise orbit determination, precise timing, aerial photogrammetry, sea level monitoring, GNSS meteorology and seismic hazard warning etc [3, 5, 7, 9, 18, 21, 23, 28].

The PPP technology can provide centimeter to decimeter, or even millimeter-level positioning accuracy under 'clear sky' conditions using a Kalman filter (KF), which is regarded as an optimal estimator [8, 13]. However, the performance (continuity, accuracy and reliability) of PPP solution using Kalman filtering rely heavily on the correct definition of both the functional and stochastic models used in the filtering process [4, 22]. To achieve the desired accuracy, a large number of researches have investigated for the PPP functional models over the past decades. The ionosphere-free code and carrier phase combinations are the most famous formulations used to alleviate the cumbersome effect caused by the ionosphere. Zumberge *et al* [30] as well as Kouba and Héroux [16] have used these combinations as the functional mode for PPP. To weaken the

observation noises, Gao and Shen [7] have proposed the UofC (University of Calgary) model which uses an average of code and carrier phase observations on L_1 and L_2 in addition to the traditional ionosphere-free combinations. To be able to extract (or derive) the absolute ionospheric delay with the use of high-precision carrier phases, some scholars have adopted the zero-difference and uncombined observations directly as the functional model for PPP [1, 2, 17, 27]. Whilst the functional models for PPP are sufficiently known and well documented in the current literature, the stochastic modeling is still a critical issue to be investigated. A good *a priori* knowledge of the process and measurement information depends on factors such as the type of application and process dynamics, which are difficult to obtain. Also, the estimation environment in the case of kinematic applications is not always fixed but is subject to change [19]. Insufficient knowledge of *a priori* filter statistics will on the one hand reduce the precision of the PPP estimates or introduce biases to their estimates. In addition, wrong *a priori* information will even lead to a failure of PPP solution.

Recently, adaptive robust filtering has received considerable attention and been a matter of interest in many studies, including Mohamed and Schwarz [19], Yang *et al* [25, 26], Ding *et al* [6], Nie *et al* [20] and Guo *et al* [10]. Applications of adaptive robust Kalman filtering techniques in GNSS (and GNSS/INS) navigation have shown encouraging results. Therefore, we present an adaptive robust Kalman filtering for PPP data processing aiming for improved performances. In order to assess its effectiveness, PPP results from several test cases using conventional Kalman filter and adaptive robust Kalman filter respectively are shown in this paper.

2. Basic models of precise point positioning

2.1. Observation model

The most popular ionosphere-free combinations of dual-frequency code and carrier phase observations are used to form PPP observation model. For the sake of simplicity, the observation model is illustrated in the following equations:

$$\begin{aligned} P_{\mathrm{IF}} &= \frac{f_1^2}{f_1^2-f_2^2}P_1 - \frac{f_2^2}{f_1^2-f_2^2}P_2 \\ &= \rho + c\cdot \mathrm{d}t + d_{\mathrm{trop}} + d^s_{\mathrm{hd}(P(L_1,L_2))} - d_{r(\mathrm{hd}(P(L_1,L_2)))} \\ &\quad + d_{\mathrm{mult}(P(L_1,L_2))} + \varepsilon_{P(L_1,L_2)} \end{aligned} \tag{1}$$

$$\begin{aligned} \Phi_{\mathrm{IF}} &= \frac{f_1^2}{f_1^2-f_2^2}\Phi_1 - \frac{f_2^2}{f_1^2-f_2^2}\Phi_2 \\ &= \rho + c\cdot \mathrm{d}t + d_{\mathrm{trop}} + N_{\mathrm{IF}} + B_{\mathrm{IF}} + d^s_{\mathrm{hd}(\Phi(L_1,L_2))} \\ &\quad - d_{r(\mathrm{hd}(\Phi(L_1,L_2)))} + d_{\mathrm{mult}(\Phi(L_1,L_2))} + \varepsilon_{\Phi(L_1,L_2)} \end{aligned} \tag{2}$$

where P_{IF} is the ionosphere-free combinations of P_1 and P_2 pseudoranges, Φ_{IF} is the ionosphere-free combinations of Φ_1 and Φ_2 carrier phases (in units of distance), ρ is the geometric range between receiver and satellite, c is the speed of light in vacuum, $\mathrm{d}t$ is receiver clock error, d_{trop} is tropospheric delay, $d^s_{hd(\cdot)}$ and $d_{r(\mathrm{hd}(\cdot))}$ is respectively the satellite and receiver hardware bias, N_{IF} is the integer phase ambiguity of the ionosphere-free phase combination, B_{IF} is the initial phase of the satellite oscillator, $d_{\mathrm{mult}(\cdot)}$ and ε are the multipath effect and measurement noise.

The traditional PPP functional model as illustrated in equations (1) and (2) is capable of mitigating the first order ionospheric delay as well as the inter-frequency bias, whereas the equipment hardware delay will remain. For the carrier phase, the nonzero initial phase will not be cancelled in these equations and will be mapped to the ambiguities. This mapping should not be a problem because the ionosphere-free ambiguities are calculated as a lumped term and treated as a float number. The estimates of PPP herein are three positional parameters, receiver clock offset, zenith tropospheric delay, and the ionosphere-free phase ambiguities. To achieve the best positioning accuracy possible, effects such as Sagnac effect, tide errors, carrier phase wind-up and transmitter antenna phase center offset must be corrected using models. Interested readers can refer to e.g. Zumberge *et al* [30], Kouba and Hérous [16] and Kouba [15] for a full parameterization discussion.

2.2. Dynamic model

The Kalman filer adopts state vector to describe the evolution (or process) of a dynamic system, and only the estimated states from the previous time step are needed to compute the predicted estimates for the current epoch. Let the linear dynamic system be given by

$$X_k = \Phi_{k,k-1}X_{k-1} + \Gamma_{k-1}W_{k-1} \tag{3}$$

where $\Phi_{k,k-1}$ denotes the state transition matrix, X_{k-1} and X_k are the previous estimates and current state vector, respectively, which consists of six types (position, velocity, acceleration, receiver clock offset, tropospheric delay and phase ambiguities) of unknown parameters as shown in equation (4)., Γ_{k-1} is the driving matrix and W_{k-1} is a process noise term.

$$X = \left[\underbrace{x,\ y,\ z}_{X_{\mathrm{pos}}},\ \overbrace{\dot{x},\ \dot{y},\ \dot{z}}^{X_{\mathrm{vel}}},\underbrace{\ddot{x},\ \ddot{y},\ \ddot{z}}_{X_{\mathrm{acc}}},\ \overbrace{\mathrm{d}t}^{X_{\mathrm{clk}}},\underbrace{\mathrm{trop}}_{X_{\mathrm{trp}}},\ \overbrace{N_1,\ \cdots N_n}^{X_{\mathrm{amb}}}\right]^T \tag{4}$$

A constant velocity (CV) model or a constant acceleration model (CA) is often used as a dynamic model of a tracking filter. Generally, the CV model can be used to satisfy the transition accuracy if the observation sampling rate is 10 Hz or even higher, otherwise the CA model should be used for state transition [24]. Considering the sampling rate of observation data is sometimes 1 Hz or even lower in practical applications, the CA model is used herein to describe the moving state evolution. The receiver clock offset and zenith tropospheric delay are usually modeled as a random walk or first order Gauss Markov process, while the ambiguities are assumed to be constants if no cycle slips occur over time [14, 16]. For illustration purpose, the state vector is divided into two parts as

shown in equation (5), and the dynamic models are given by equations (6) and (7).

$$X = [X_{\text{state}} \quad X_{\text{other}}]^T;\ W = [W_{\text{state}} \quad W_{\text{other}}]^T \tag{5}$$

$$X_{\text{state}} = \begin{bmatrix} X_{\text{pos}} \\ \dot{X}_{\text{vel}} \\ \ddot{X}_{\text{acc}} \end{bmatrix}_k = \begin{bmatrix} I_{3\times3} & \Delta t \cdot I_{3\times3} & \Delta t^2/2 \cdot I_{3\times3} \\ 0_{3\times3} & I_{3\times3} & \Delta t \cdot I_{3\times3} \\ 0_{3\times3} & 0_{3\times3} & I_{3\times3} \end{bmatrix} \begin{bmatrix} X_{\text{pos}} \\ \dot{X}_{\text{vel}} \\ \ddot{X}_{\text{acc}} \end{bmatrix}_{k-1} + \begin{bmatrix} 0_{3\times3} \\ 0_{3\times3} \\ I_{3\times3} \end{bmatrix} W_{\text{state}}(k) \tag{6}$$

$$X_{\text{other}} = \begin{bmatrix} X_{\text{clk}} \\ X_{\text{trp}} \\ X_{\text{amb}} \end{bmatrix}_k = \begin{bmatrix} 1 & 0 & 0 \\ 0 & 1 & 0 \\ 0 & 0 & I_{n\times n} \end{bmatrix} \begin{bmatrix} X_{\text{clk}} \\ X_{\text{trp}} \\ X_{\text{amb}} \end{bmatrix}_{k-1} + \begin{bmatrix} 1 \\ 1 \\ 0_{n\times n} \end{bmatrix} W_{\text{other}}(k) \tag{7}$$

where X_{state} denotes the moving state parameters, which covers the vehicle's position, velocity and acceleration; X_{other} represents the remaining parameters, which contains the receiver clock offset, zenith tropospheric delay and ambiguities; W_{state} and W_{other} are the corresponding process noise vectors; I is an identity matrix, Δt is the sampling interval.

2.3 Stochastic model

A proper modeling of PPP must guarantee an incorporation of statistical information along with its deterministic component. Two branches of stochastic modeling are addressed: observations and system dynamic.

Stochastic modeling of observation includes information about the accuracy of measurements used in PPP and any relations among them. As most of the dual frequency receivers tend to be codeless, the weight matrix or covariance matrix of undifferenced PPP will be diagonal and the value of the diagonals will mainly depend on the measurement accuracy. The measurements' accuracy can be quantified through either the elevation of the satellite, the signal to noise ration, or a combination of both. The stochastic model of the observation used herein is a cosine function

$$\sigma^2 = a^2 + b^2 \cos^2 E \tag{8}$$

where σ^2 is the variance of measurement noise, E is the satellite elevation angle, a, b are empirical coefficients, generally taken to be 0.003 for the carrier phase measurements.

The stochastic description of the system dynamics expresses the kinematic behavior of the vehicle and the evolution of parameters with time. Assuming the acceleration rate is a white noise process with constant spectral density, the covariance matrix of the system noise (process noise) as shown in equation (9) can be deduced from the solution of the differential equation of the system dynamic and the propagation of its covariance matrix.

$$Q_{\text{state}} \approx \begin{bmatrix} \frac{\Delta t^4}{20} I_{3\times3} & \frac{\Delta t^3}{8} I_{3\times3} & \frac{\Delta t^2}{6} I_{3\times3} \\ \frac{\Delta t^3}{8} I_{3\times3} & \frac{\Delta t^2}{3} I_{3\times3} & \frac{\Delta t}{2} I_{3\times3} \\ \frac{\Delta t^2}{6} I_{3\times3} & \frac{\Delta t}{2} I_{3\times3} & I_{3\times3} \end{bmatrix} \sigma_a^2 \tag{9}$$

where σ_a^2 is a constant variance, which should be determined according to the vehicle's maneuvering and disturbances. For static PPP, it can be set to 0 since the speed and acceleration of the target are exactly known.

3. Adaptively robust Kalman filtering

3.1. Recursive algorithm

We start with the discrete linear system,

$$\begin{cases} L_k = H_k X_k + e_k \\ X_k = \Phi_{k,k-1} X_{k-1} + \Gamma_{k-1} W_{k-1} \end{cases} \tag{10}$$

where $X_k \in \Re^n$ denotes state vector at epoch t_k, $L_k \in \Re^m$ is measurement vector, $\Phi_{k,k-1}$ is state transition matrix, H_k is observation (design) matrix, Γ_{k-1} is noise drive matrix. W_k and e_k are respectively the process noise and measurement noise vector, which are assumed to be uncorrelated Gaussian white noise with zero mean and covariance Q_k and R_k.

In order to resist the influences of both measurement outliers and state model errors, an adaptive robust filter is developed by combining the adaptive Kalman filter and robust estimation. The main feature of this filter consists in introducing an equivalent weight matrix (or equivalent covariance matrix) to compensate the observational outliers, and an adaptive factor to control the state turbulences. Therefore, the adaptive robust Kalman filter can be derived by the following Lagrangian optimization condition [25]

$$\Omega = (H_k \widehat{X}_k - L_k)^T \overline{R}_k^{-1} (H_k \widehat{X}_k - L_k) + \alpha_k (\widehat{X}_k - \widehat{X}_{k,k-1})^T P_k^{-1} (\widehat{X}_k - \widehat{X}_{k,k-1}) = \min \tag{11}$$

where $\overline{R}_k$ denotes the equivalent covariance matrix of measurement noise, α is an adaptive factor ($0 < \alpha \leq 1$), $\widehat{X}_{k,k-1}$ is the predicted state vector, $\widehat{X}_k$ and P_k are the updated state vector and its covariance matrix, respectively.

Giving the system's initial state vector and covariance matrix $\widehat{X}_0$ and P_0, the state vector and its covariance matrix of any epoch can be calculated by solving equation (11). For simplicity, the recursive equations of the adaptive robust KF take the following general form

$$\widehat{X}_{k,k-1} = \Phi_{k,k-1} \widehat{X}_{k-1} \tag{12}$$

$$P_{k,k-1} = \Phi_{k,k-1} P_{k-1} \Phi^T{}_{k,k-1} + \Gamma_{k-1} Q_{k-1} \Gamma^T{}_{k-1} \tag{13}$$

$$K_k = \frac{1}{\alpha_k} P_{k,k-1} H_k^T \left(\frac{1}{\alpha_k} H_k P_{k,k-1} H_k^T + \overline{R}_k \right)^{-1} \tag{14}$$

$$\widehat{X}_k = \widehat{X}_{k,k-1} + K_k(L_k - H_K\widehat{X}_{k.k-1}) \quad (15)$$

$$P_k = (I - K_kH_k)P_{k,k-1}(I - K_kH_k)^T + K_k\overline{R}_kK_k^T \quad (16)$$

where $\widehat{X}_k$ and $\widehat{X}_{k\text{-}1}$ are the estimated state vector at epoch t_k and $t_{k\text{-}1}$, K_k is the filter gain matrix, which defines the updating weight between new measurements and predictions from the system dynamic model, I is an identity matrix.

It is easily observed that the algorithm of the adaptive robust KF is consistent with the conventional KF from the perspective of recursive form. The only difference lies in the computation of the filter gain matrices. If the filtering is contaminated by outliers, the equivalent covariance ($\overline{R}_k$) instead of the original covariance (R_k) is used for controlling the observational outliers. Furthermore, an adaptive factor (α_k) is used to balance the dynamic model information and the measurements.

3.2. Determination of the equivalent covariance matrix and adaptive factor

To obtain the optimal solution from adaptive robust Kalman filter, we need to compute the equivalent covariance matrix and adaptive factor at first. The Huber weight function [12], Hampel function, Turkey bi-weight function [11] or a so-called IGG (Institute of Geodesy and Geophysics) III function [26, 29] are commonly used for calculating the equivalent covariance matrix. In the case of undifferenced PPP, the observational covariance matrix is a diagonal matrix because of the independence of the observations. Herein an improved iterative robust filtering scheme is used to adjust the variance of observations according to IGG III function [26]

$$\overline{R}_i = R_i/\gamma_i \quad (17)$$

$$\gamma_i = \begin{cases} 1 & |\widetilde{v}_i| \le k_0 \\ \dfrac{k_0}{|\widetilde{v}_i|}\left(\dfrac{k_1 - |\widetilde{v}_i|}{k_1 - k_0}\right)^2 & k_0 < |\widetilde{v}_i| \le k_1 \\ 0 & |\widetilde{v}_i| > k_1 \end{cases} \quad (18)$$

where γ_i is the variance inflation factor, $\widetilde{v}_i$ is the standardized residual, k_0 and k_1 are two thresholds, which are usually chosen as $k_0 = 1.5\text{~}3.0$ and $k_1 = 3.0\text{~}8.0$. As illustrated in equations (17) and (18), the equivalent variance function shows three segments: if the residual is small enough, the equivalent variance equals to the original variance; if the residual is relative large but reasonable, the equivalent variances are moderately flatted; and if the residuals are significant large and unacceptable, the equivalent variance approaches infinity (equivalent to be removed). Compared with the conventional robust estimation, the improved robust filtering does not conduct equivalent variance function simultaneously for all observations. Only the observation with largest standardized residual will be operated by the IGG III function in each iteration to avoid reducing the contribution of the normal observations or even filter divergence.

An appropriate adaptive factor should be sensitive to the disturbances of the predicted parameters or the dynamic model errors. Both posterior residual and predicted residual (innovations) can be used to construct the adaptive factor. However, when both the measurements and dynamic model are distorted by outliers, the filter cannot distinguish them and the adaptive factor will be influenced by the posterior residuals. In addition, the posterior residual-based adaptive factor may not be obtained when lack of enough observations. Herein an innovation-based statistic $\overline{V}_{k,k-1}$ is constructed and a three-segment function similar to the IGG III scheme is presented for adaption.

$$\overline{V}_{k,k-1} = \frac{\sum_{i=1}^{n_k} \widetilde{v}^2{}_{k,k-1}}{\sum_{i=1}^{n_k} \sigma^2_{v_{k,k-1}}} \quad (19)$$

$$\alpha_k = \begin{cases} 1 & \left|\overline{V}_{k,k-1}\right| \le c_0 \\ \dfrac{c_0}{\left|\overline{V}_{k,k-1}\right|}\left(\dfrac{c_1 - \left|\overline{V}_{k,k-1}\right|}{c_1 - c_0}\right)^2 & c_0 < \left|\overline{V}_{k,k-1}\right| \le c_1 \\ 0 & \left|\overline{V}_{k,k-1}\right| > c_1 \end{cases} \quad (20)$$

where c_0 and c_1 are two constants with experienced values $c_0 = 1.5\text{~}3.0$, $c_1 = 3.0\text{~}8.0$; $\widetilde{v}_{k,k-1}$ is the innovation and $\sigma_{v_{k,k-1}}$ is the standard deviation of $\widetilde{v}_{k,k-1}$; n_k is the number of innovations. The adaptive factor α_k changes between 0 and 1, which balances the contribution of the new measurements and the updated parameters to the new estimates. It should be noted that this adaptive factor controls the dynamic error as a whole rather than consider the error influence of the individual elements. The biggest advantage of this approach is that it will not damage the correlation between state parameters because of the synchronized scaling covariance. Also, it achieves a consistent form with the equivalent covariance model which makes it more convenient for practical implementation.

4. Validation tests

To illustrate the effectiveness of adaptive robust Kalman filtering, both static and kinematic PPP were performed. Products such as precise satellite orbit, clock error, and differential code bias required for PPP were provided by the community of International GNSS Service (IGS, available at: http://igsws.unavco.org/components/prods.html, 1 July, 2014). For comparison, the following two schemes are designed.

Scheme 1: classic Kalman filtering (KF), i.e. $\overline{R}_k = R_k$ and $\alpha_k = 1$.

Scheme 2: adaptive robust Kalman filtering (ARKF), i.e. $\overline{R}_k$ is determined by equations (17) and (18) and α_k is determined by equations (19) and (20).

Table 1. Root mean square of static PPP positioning biases (m) and improvements (%).

	ADIS	DUM1	JPLM	KOUR	MATE	NANO	NICO	VILL	ZECK
Scheme 1	0.053	0.025	0.030	0.053	0.047	0.019	0.028	0.008	0.032
Scheme 2	0.028	0.016	0.024	0.018	0.024	0.011	0.007	0.003	0.016
Improvement (%)	47.2	36.0	20.0	66.1	48.9	42.1	75.0	62.5	50.0

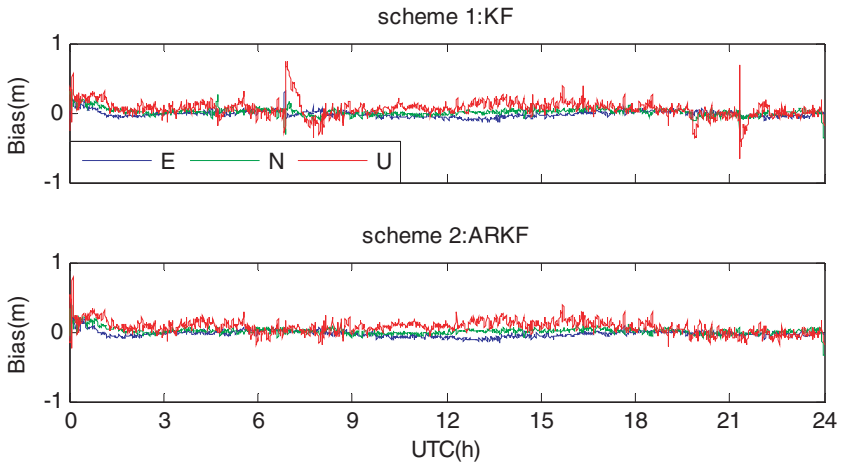

Figure 1. Time series of epoch-wise PPP positioning error at HOB2.

4.1. Static PPP solution

Approximately one hundred globally distributed IGS reference stations were selected for daily (24 h) static PPP solution using the above two schemes. Results show that solutions with different schemes agree with each other very well for most of the sites, and only a few solutions differ greatly. Table 1 lists the corresponding 3D positioning biases of several stations, on which notable differences can be observed.

For most (~90%) static PPP experiments, there is no significant difference (improvements less than 10%) between the two filtering solutions. This is reasonable when we acknowledge the fact that static GNSS data are less susceptible to the unexpected observational error and dynamic interference. In addition, smoothing algorithms with a long time static observations will further weaken the bad influence of any unknown error. Anyway, the adaptive robust Kalman filter does improve the performances of static PPP as shown in table 1, particularly for NICO and KOUR2. Compared with the classic Kalman filter, the mean improvement of the adaptive robust Kalman filter reaches nearly 50% for these nine stations.

4.2. Simulated kinematic PPP solution

A set of static GPS data recorded on 1st June 2012 at a reference station (HOB2) were used for epoch-wise PPP solution using the above two filtering schemes. The corresponding positioning biases including the east (E), north (N) and up (U) components are shown in figure 1.

It can be observed that the positioning error varies by less than 0.2 m in horizontal and 0.5 m in vertical direction for most of the epochs. There is no significant discrepancy between the positioning accuracy of both the classic Kalman filter and adaptive robust Kalman filter with clean data. However, once the observations are contaminated by unexpected outliers (e.g. gross errors, cycle slips), large variations up to 1 m can be observed during the periods 6:00–9:00 UT and 20:00–22:00 using classic Kalman filter. On the contrary, smoothly running and accurate positioning results can be obtained even under poor conditions when the adaptive robust Kalman filtering scheme was applied for epoch-wise PPP solution. The reason for this may attribute to the equivalent variance matrix, which balances the contribution of the normal and abnormal observations.

4.3. Airborne kinematic PPP solution

Further validations have been performed for real kinematic scenes. Take a flight test for example. GPS Data recorded on 28th April 2011 (generated at 1 s interval for 1.5 h) were used for epoch-wise PPP solution. Simultaneously, the data of the airplane were processed in double differenced (DD) mode with respect to a base station to produce the reference solution using GrafNav software, which is developed by the Waypoint Products Group of NovAtel. The positioning results obtained from PPP were compared with the 'true values' from DD processing that has a positioning accuracy better than 10 cm and characterized with successful ambiguity fixing. Figure 2 shows the horizontal trajectory of the flight and its variation over time. Figure 3 shows the corresponding positioning error with the above two mentioned filtering schemes.

As shown in figure 2, the airplane turns frequently in the plane direction with high-dynamic maneuvering. Consequently, the positioning accuracy of scheme 1 as shown in the upper plot of figure 3 dramatically decreases once the airplane is experiencing acceleration or deceleration. This is particularly significant when the airplane takes off or turns around. The reason for this may be attributed to the following two aspects: firstly, the quality of received data is more vulnerable to be

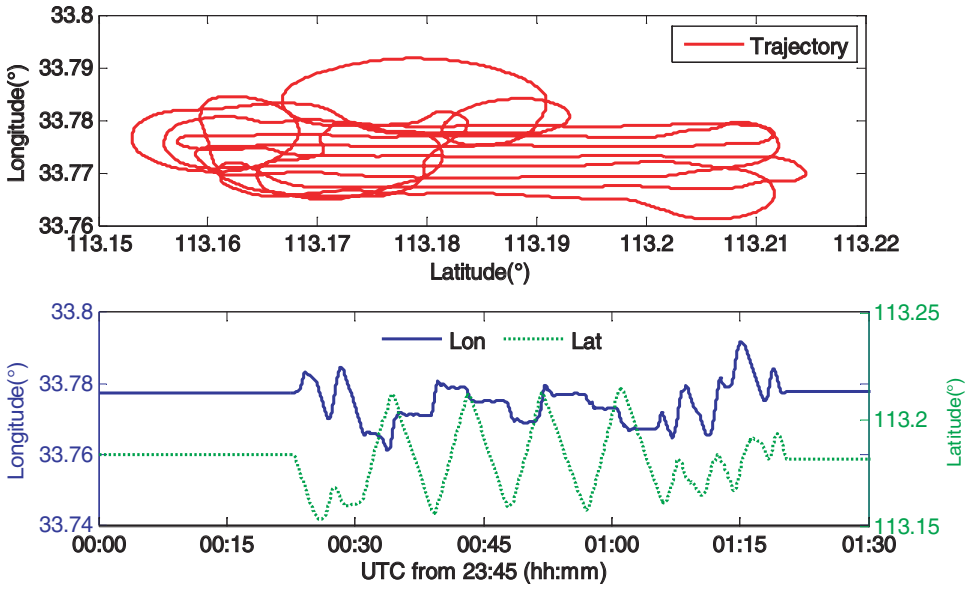

Figure 2. Horizontal trajectory of the flight (upper plot) and its variation over time (lower plot).

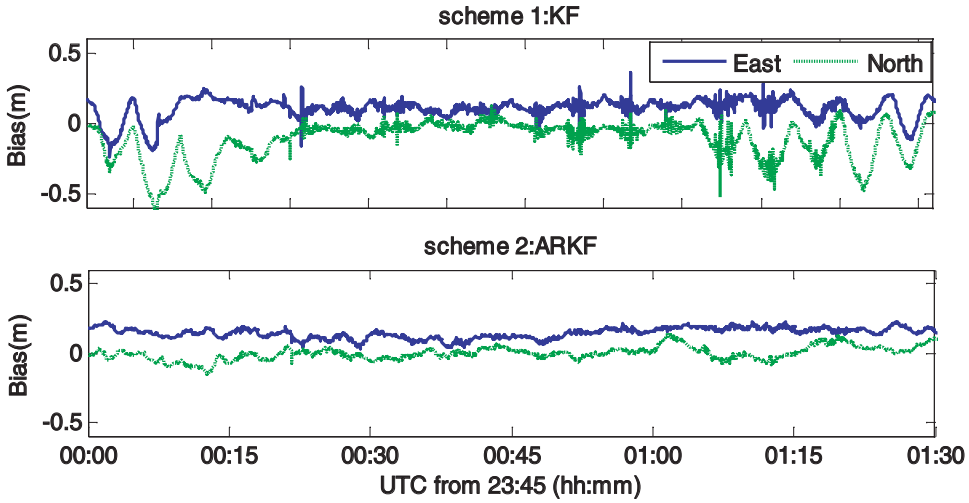

Figure 3. Time series of the positioning error for the flight test using different filtering schemes.

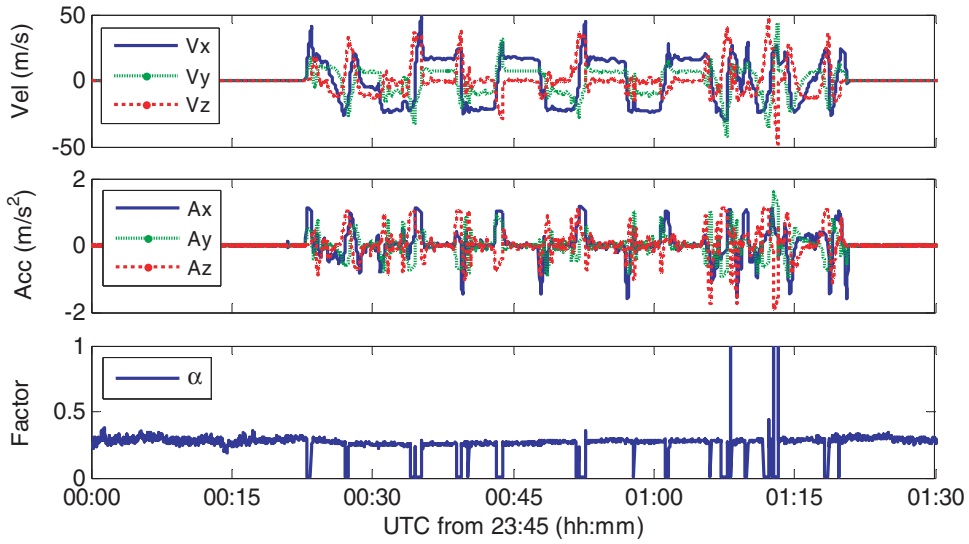

Figure 4. Coordinate relation between adaptive factor and estimated velocity/acceleration.

affected by various outliers under these circumstances. When the airplane takes off or turns around, the view to the sky may change rapidly or even be obscured by the wing or fuselage of the plane. This may cause inevitable data interference due to cycle slips, gross errors and loss-of-lock, and consequently degrades the performance of PPP solution. Secondly, the given CA dynamic model is no longer adaptive to the actual situation for a disorganized maneuvering target. Due to the discrepancy between the real maneuvering and the dynamic model, giving inappropriate (overestimated) weights to the predictions will inevitably deteriorate the tracking performance of PPP using the classic Kalman filtering. In contrast, the lower plot of figure 3 shows that much more smooth and accurate positioning results were obtained during the whole periods when the adaptive robust Kalman filtering scheme was applied in kinematic PPP solution. This is reasonable taking into account that the adaptively robust Kalman filter couples an equivalent covariance matrix and an adaptive factor to balance the contribution of observational information and dynamic information. It cannot only resist the influence of measurement outliers, but also controls the effects of complex kinematic model errors.

To intuitively investigate how the adaptive factor controls the dynamic disturbances, the coordinate relation between adaptive factor and estimated velocity/acceleration is given in figure 4. The upper two plots show respectively the velocities and accelerations of the airplane, and the lower one shows the corresponding adaptive factors.

As illustrated in figure 4, the curves of velocity, acceleration and adaptive factor run smoothly during the stationary and stable flying states. However, sudden changes of velocity and acceleration can be observed once the airplane takes off or turns around, and the adaptive factor sharply drops to near zero. In this case the updated parameters will mainly depend on the contribution of observational information. Due to the lack of enough observations, sudden increase of adaptive factor to near 1 can be noticed in the lower plot of figure 4, and the updated parameters will mainly depend on the contribution of system dynamic information in this case. Herein it is worth mentioning that the values of adaptive factor are relatively small (0.2 ~ 0.3), which means the given dynamic model does not confirm the moving process very well. Therefore, to further enhance the performance of PPP, future in-depth studies should be devoted to this problem.

5. Conclusions

An innovation-based adaptive robust Kalman filtering is developed for PPP processing. To illustrate the performance and superiority of adaptive robust Kalman filtering, both classic Kalman filtering and adaptive robust Kalman filtering schemes are designed for PPP solution with static and kinematic modes. Experimental results show that the adaptive robust Kalman filter outperforms the classic Kalman filter by tuning either the system noise variance-covariance matrix or the updated measurement noise variance-covariance matrix or both of them. This implies that the adaptive robust Kalman filter cannot only resist gross errors of observation data, but also control unexpected state turbulences. This makes it valuable in PPP processing, particularly for moving target tracking with complex maneuvering. However, a problem worthy to be pointed out is that the single-adaptive-factor based filtering used in this paper controls the state turbulences as a whole neglecting distinguish the adaption of different types of parameters. The currently developed classified adaptive robust Kalmam filtering provides us a new solution. On the other hand, the commonly used CV (Constant Velocity) or CA (Constant Acceleration) dynamic models may be invalid if a moving target turns due to the disagreement between the real dynamic and these models. Further in-depth studies should be devoted to these problems.

Acknowledgments

The authors gratefully acknowledge IGS community for providing global GNSS data and products. We also appreciate two anonymous reviewers and the editor in chief for their valuable comments and improvements to this manuscript. This study was supported by the China Postdoctoral Science Foundation (No. 133280) and International Postdoctoral Exchange Fellowship Program 2013 by the Office of China Postdoctoral Council (No. 2013042).

References

[1] Abdel-salam M 2005 Precise point positioning using un-differenced code and carrier phase observations (Canada: University of Calgary) *UCGE Reports No. 20229*

[2] Abdel-salam M and Gao Y 2004 Precise GPS atmosphere sensing based on un-differenced observations *Proc. 17th Int. Technical Meeting of the Satellite Division of The Institute of Navigation (ION GNSS 2004)* September 21–24 (Long Beach, California, USA) 933–40

[3] Bisnath S and Gao Y 2007 Current state of precise point positioning and future prospects and limitations *Proceedings of IUGG 24th General Assembly* July 2–13 (Perugia, Italy)

[4] Brown R G and Hwang P Y C 1992 *Introduction to Random Signals and Applied Kalman Filtering* (New York: John Wiley)

[5] Chen W, Hu C, Li Z, Chen Y, Ding X, Gao S and Ji S 2004 Kinematic GPS precise point positioning for sea level monitoring with GPS buoy *J. Global Positioning Syst.* **3** 302–7

[6] Ding W, Wang J and Rizos C 2007 Improving adaptive Kalman estimation in GPS/INS integration *J. Navig.* **60** 517–29

[7] Gao Y and Shen X 2001 Improving ambiguity convergence in carrier phase-based precise point positioning *Proc. 14th Int. Technical Meeting of the Satellite Division of The Institute of Navigation (ION GPS 2001)* September 11–14 (Salt Lake City, UT, USA) 1532–9

[8] Gelb A 1974 *Applied Optimal Estimation* (Cambridge, MA: MIT Press)

[9] Geng J, Teferle FN, Meng X and Dodson AH 2010 Kinematic precise point positioning at remote marine platforms *GPS Solutions* **14** 343–50

[10] Guo F, Zhang X and Li X 2013 Adaptive robust Kalman filter for kinematic precise point positioning *Proc. IAG Scientific Assembly* 1–6 September (Potsdam, Germany)

[11] Hampel F, Ronchetti E, Rousseeuw P and Stahel W 1986 *Robust Statistics. The Approach Based on Influence Functions* (New York: Wiley)
[12] Huber P J 1981 *Robust Statistics* (New York: John Wiley)
[13] Kalman R E 1960 A new approach to linear filtering and prediction problems *Trans. ASME* **82** 35–45
[14] Kechine M, Tiberius C and Marel H 2003 Experimental verification of internet-based global differential GPS *Proc. ION GPS 2003* 24–27 September (Portland, Oregon)
[15] Kouba J 2009 A guide to using international GNSS service (IGS) products (http://acc.igs.org/UsingIGSProductsVer21.pdf)
[16] Kouba J and Héroux P 2001 Precise point positioning using IGS orbit and clock products *GPS Solutions* **5** 12–28
[17] Li W, Cheng P and Bi J 2011 Regional ionosphere delay's calibration and accuracy assessment based on un-combined precise point positioning *Geo. Inf. Sci. Wuhan University* **36** 1200–3
[18] Li X, Ge M, Zhang X, Zhang Y, Guo B, Wang R, Klotz J and Wickert J 2013 Real-time high-rate coseismic displacement from ambiguity-fixed PPP: application to earthquake early warning *Geophys. Res. Lett.* **40** 1–6
[19] Mohamed A H and Schwarz K P 1999 Adaptive Kalman filtering for INS/GPS *J. Geod.* **73** 193–203
[20] Nie J, Zhang S, Xu Y, Zhang Y and Wang Y 2010 Precise point positioning based on Robust Kalman filtering *J. Earth Sci. Environ.* **32** 218–20 (in Chinese)
[21] Shi C, Lou Y, Zhang H, Zhao Q, Geng J, Wang R, Fang R and Liu J 2010 Seismic deformation of the Mw 8.0 Wenchuan earthquake from high-rate GPS observations *Adv. Space Res.* **46** 228–35
[22] Wang J, Satirapod C and Rizos C 2002 Stochastic assessment of GPS carrier phase measurements for precise static relative positioning *J. Geod.* **76** 95–104
[23] Xu P, Shi C, Fang R, Liu J, Niu X, Zhang Q and Yanagidani T 2013 High-rate precise point positioning (PPP) to measure seismic wave motions: an experimental comparison of GPS PPP with inertial measurement units *J. Geod.* **87** 361–72
[24] Yang Y 2006 *Adaptive Navigation and Kinematic Positioning* (Beijing: Press of Surveying and Mapping) ISBN 7-5030-1661-2
[25] Yang Y, He H and Xu G 2001 Adaptively robust filtering for kinematic geodetic positioning *J. Geod.* **75** 109–16
[26] Yang Y, Song L and Xu T 2002 Robust estimator for correlated observations based on bifactor equivalent weights *J. Geod.* **76** 353–8
[27] Zhang B, Ou J, Yuan Y and Zhong S 2010 Precise point positioning algorithm based on original dual-frequency GPS code and carrier-phase observations and application *Acta Geodaetica et Cartographica Sinica* **39** 478–83
[28] Zhang X H and Andersen O B 2006 Surface ice flow velocity and tide retrieval of the Amery ice shelf using precise point positioning *J. Geod.* **80** 171–6
[29] Zhu J 1996 Robustness and the robust estimate *J. Geod.* **70** 586–90
[30] Zumberge J F, Heflin M B, Jefferson D C, Watkins M M and Webb F H 1997 Precise point positioning for the efficient and robust analysis of GPS data from large networks *J. Geophys. Res.* **102** 5005–17